Available online at www.sciencedirect.com
ScienceDirect
Journal of Hazardous Materials 157 (2008) 79–87
Journal of Hazardous Materials
www.elsevier.com/locate/jhazmat

Effect of activated carbon fiber anode structure and electrolysis conditions on electrochemical degradation of dye wastewater

Fenyun Yi [a], Shuixia Chen [a,b,*], Chan'e Yuan [a]

[a] *PCFM Laboratory, OFCM Institute, School of Chemistry and Chemical Engineering, Sun Yat-Sen University, Guangzhou 510275, PR China*
[b] *Materials Science Institute, Sun Yat-Sen University, Guangzhou 510275, PR China*

Received 6 October 2007; received in revised form 8 December 2007; accepted 20 December 2007
Available online 4 January 2008

Abstract

The alizarin red S (ARS) in simulated dye wastewater was electrochemically oxidized using an activated carbon fiber (ACF) felt as an anode. The influence of electrolytic conditions and anode structure on the dye degradation was investigated. The results indicated that initial pH, current density and supporting electrolyte type all played an important role in the dye degradation. The chemical oxygen demand (COD) removal efficiency of dye solution in neutral or alkaline medium was about 74% after 60 min of electrolysis, which was higher than that in acidic medium. Increasing current density would lead to a corresponding increase in the dye removal. The addition of NaCl could also improve the treatment effect by enhancing the COD removal efficiency 10.3%. For ACF anodes, larger specific surface area and higher mesopore percentage could ensure more effective electrochemical degradation of dye. The data showed that the color removal efficiency increased from 54.2 to 83.9% with the specific surface area of ACF anodes increasing correspondingly from 894 to 1682 m^2/g.

Keywords: Activated carbon fiber; Electrochemical oxidation; Alizarin red S; Dye wastewater

1. Introduction

Dye wastewater is characterized by large amounts of discharge, high concentration, complicated composition and high chroma [1]. Conventional dye wastewater treatment methods are gradually becoming inadequate to meet the requirements of a higher environmental quality. In recent years, various advanced oxidation processes such as ozonation [2], wet air oxidation [3,4], supercritical water oxidation [5], photocatalytic oxidation [6,7], electrochemical oxidation [8–11] and other integrated techniques [12–14] have been proposed as substitutes for the conventional treatment techniques. Among these advanced oxidation processes, electrochemical oxidation method which uses electrons as the main reagent, only requiring a little or even no chemical reagent, is a clean and effective wastewater treatment method.

Recently, there has been an increasing interest in the application of electrochemical oxidation method for the wastewater treatment. Moreover, more and more attention has been focused on the exploration of novel anodes where the degradation of organic compounds mostly happens. At present, graphite electrode [15], iron electrode [16,17], PbO_2 electrode [18], noble metal electrode [19,20], dimensionally stable anode (DSA) [10,21-22] and boron doped diamond electrode (BDD) [8,9,23–25] are usually used as the anode in the electrochemical oxidation. Among them, the recently developed DSA and BDD are generally believed to be two promising anodes. Because DSA can provide high current efficiency for the oxidation of chloride ions, the use of DSA for the indirect degradation of organic pollutants is an active area of research [22]. But the active chlorine (given by the mixture of Cl_2, HOCl and OCl^-) can only lead partial mineralization of dyes. Whereas on the BDD surface, a large amount of hydroxyl radical ($OH^\bullet$) that exhibits strong oxidant properties can be formed by water oxidation, so that almost complete color removal and mineralization can be obtained by using BDD electrodes. Panizza and Cerisola [26] compared the catalytic activities of four electrode materials (i.e., $TiRuSnO_2$, Pt, PbO_2 and BDD) for the anodic oxidation of methyl red. The bulk

* Corresponding author at: Materials Science Institute, Sun Yat-Sen University, Guangzhou 510275, PR China. Tel.: +86 20 84112093; fax: +86 20 84034027.
E-mail address: cescsx@mail.sysu.edu.cn (S. Chen).

0304-3894/$ – see front matter © 2007 Elsevier B.V. All rights reserved.
doi:10.1016/j.jhazmat.2007.12.093

electrolysis showed that the complete COD and color removal were only achieved using PbO_2 and BDD while $TiRuSnO_2$ and Pt only permitted a partial oxidation of methyl red. Chen et al. [27] also confirmed that the Ti/BDD electrode is much better than the $Ti/SnO_2–Sb_2O_5$ electrode for pollutant oxidation in activity and stability.

With electrochemical technology developing, the idea of three-dimensional electrodes has also been put forward [13,28]. Besides particles of the packed bed electrode and the reticulated texture of reticulated vitreous carbon electrode, the porous structure of activated carbon fiber felt can also improve mass transfer of the solution and enlarge the area of electrodes. Therefore, activated carbon fiber (ACF) that possesses high specific surface area, excellent adsorption capability, better catalytic and electric capability was introduced to the wastewater electrochemical treatment as a novel three-dimensional carbon electrode [29]. It was reported [29] that the potential for oxygen evolution on ACF electrode is 1.7 V which is approximately equal to that on platinum electrode. The electrochemical treatment of dye by using ACF as anodes can combine adsorption and electrochemical degradation of dye on the ACF anode to enhance the degradation efficiency of dye and prolong the life-span of ACF anode. Wang et al. [30] investigated the electrochemical degradation of acid red B (ARB) by using high surface area ACF as an anode or a cathode, respectively. The results show that a high concentration of active hydroxyl radicals was produced in both systems. Accordingly they concluded that the degradation of ARB on the ACF anode was attributed to direct electro-oxidation by electrogenerated hydroxyl radicals sorbed on the active sites at the ACF anode surface. Fan et al. [29] studied the degradation of Amaranth on ACF electrode under potentiostatic with electrochemical method. For the dye with the initial concentration of 80 mg/L, the COD and TOC removal ratios were about 35 and 30% by electro-oxidation. Our previous work [31] studied the feasibility of the electrochemical treatment of alizarin red S dye wastewater using an ACF as anode material. The results show that 98% of the color removal ratio and 76.5% of the maximum COD removal ratio can be obtained after 60 min of electrolysis for ARS with the initial concentration of 700 mg/L.

Few papers on the influences of the structure of ACF anode on the dye degradation have been published up to now. Based on our previous work [31], this study mostly investigated the influences of electrolytic conditions and the structure of ACF anode on the dye degradation in details. At the same time, surface structure of ACF anode after electrolysis was also analyzed.

2. Experimental

2.1. Materials and reagents

Viscose-based activated carbon fiber felts (VACFs) were prepared by carbonization and activation using viscose fiber felts as precursors, with a specific surface area in the adjusted range of 800–1700 m^2/g by controlling the activation conditions. Alizarin red S (ARS) was of analytical grade and purchased from Tianjin Xinchun Chemical Reagents Institute, China. All other reagents used were of analytical grade.

2.2. Electrolytic cell

The above prepared VACF felt was washed with distilled water, and then dried in vacuum at 110 °C. The treated VACF felt was cut into pieces with same size. Then the VACF piece was inserted between two frames and fixed. A piece of VACF felt (2 cm × 3 cm) with both faces active was used as the anode, connected to a platinum wire to ensure the electric contact. And two stainless steel plates (2 cm × 3 cm) were employed to act as the cathode. The anode was inserted between the cathodes with an interelectrode gap of 1 cm.

2.3. Electrolysis and adsorption experiments

2.3.1. Batch experiment

The batch experiment was done with 50 mL of simulated dye wastewater (containing 700 mg/L ARS and a known concentration of sodium sulfate) in the above electrolytic cell. The initial COD of the simulated dye wastewater was about 645 mg/L. The electrolysis was carried out under a constant current supplied by a DC power source, with a magnetic stirrer being used to achieve effective dispersion.

Through the batch experiments, the influences of electrolytic conditions including initial pH of solution, current density and supporting electrolyte on the dye degradation were studied. The absorbencies of the tested solutions at 507 nm were determined at different time intervals to evaluate the color removal efficiency. COD removal efficiency could be derived from COD values of original solution and treated solution after 60 min of electrolysis.

2.3.2. Continuous experiment

The experimental setup employed in this study is shown in Fig. 1. 110 mL of simulated dye wastewater (with an original pH of about 6.5, containing 200 mg/L ARS and 0.10 mol/L sodium sulfate) was filled into the electrolytic cell and treated with the VACF applied as an adsorbent in adsorption experiment

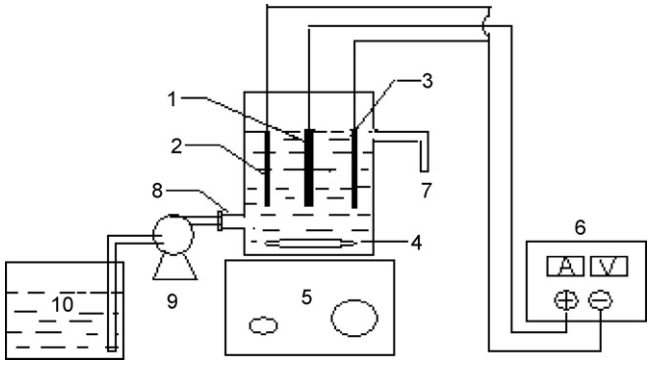

Fig. 1. Continuous experimental setup (1, VACF anode; 2, 3, stainless steel cathode; 4, magnetic bar; 5, magnetic stirrer; 6, DC power source; 7, solution exit; 8, dye wastewater entrance; 9, peristaltic pump; 10, original dye wastewater tank).

or as an anode in electrolysis experiment. The initial COD of the simulated dye wastewater was about 184 mg/L. During the treatment, the above ARS simulated dye wastewater was continuously fed into the electrolytic cell by means of a 7518-10 model Masterflex L/S peristaltic pump (Cole-Parmer Instrument Co., Ltd.) with a constant flow velocity of 2.35 mL/min. The treated solution was collected from the exit 7 (Fig. 1) every 10 min. 2.0 mL of each sample was taken. The absorbencies of the samples at 507, 331 and 259 nm were then measured, respectively.

The absorbance measurements in batch and continuous experiments were all made on a UV-7504C model UV–vis spectrophotometer (Shanghai Xinmao Instruments Co., China). COD values of dye solutions were determined according to literature [32] with a MS-3 model microwave digestion instrument (South China Environmental Science and Technology Exploitation Co., China) based on the method of acidic oxidation by dichromate.

2.4. Characterization of VACF structure

Surface chemical structure of the VACFs was characterized by reflection Fourier transform infrared spectroscopy (ATR/FTIR) determined on a Nicolet Nexus 670 FT-IR instrument (Thermo. Nicolet, Madison, WI, USA). The surface morphology of the VACFs was observed via scanning electron microscope (SEM, JSM-6330F, Japan). The Brunauer–Emmett–Teller (BET) surface area and pore volume of materials were calculated based on nitrogen adsorption isotherms measured at 77 K using an ASAP 2010 analyzer (Micromeritics, USA). The pore size distribution could also be calculated from the above nitrogen adsorption isotherm by density functional theory (DFT) method.

3. Results and discussion

3.1. Influence of electrolytic conditions on ARS degradation

3.1.1. Effect of initial pH

Fig. 2 shows the ARS removal data for five samples, each containing 700 mg/L ARS and 0.10 mol/L Na_2SO_4, with pH values (adjusted with sulfuric acid or sodium hydroxide) of 3, 5, 7, 9 and 11, respectively. And here a current density of 25 mA/cm^2 was employed. The experimental results indicate that initial pH did not obviously affect the color removal efficiency of dye solution only except at the early phase of electrolysis. While for the COD removal, an evident change caused by varied pH indeed occurred. With the initial pH increasing from 3 to 7, the COD

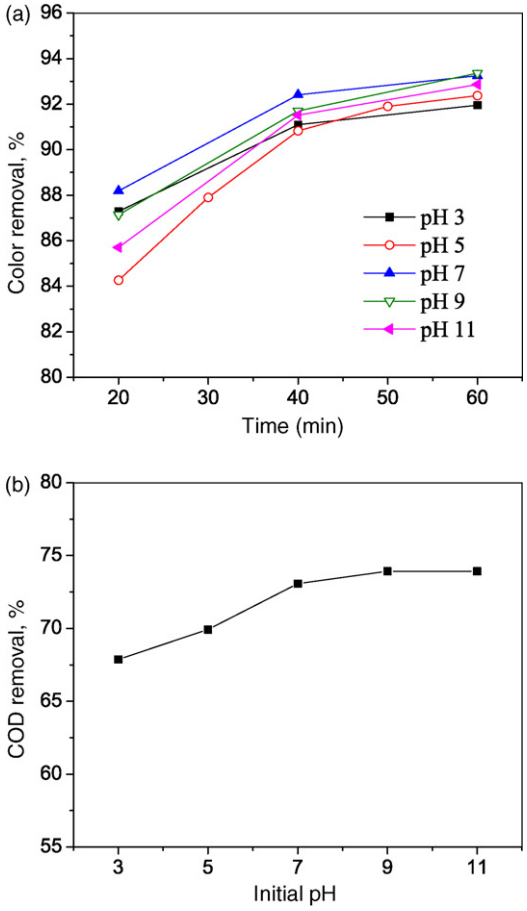

Fig. 2. Effect of initial pH on (a) the color removal and (b) the COD removal (ARS initial concentration, 700 mg/L; Na_2SO_4 concentration, 0.10 mol/L; current density, 25 mA/cm^2).

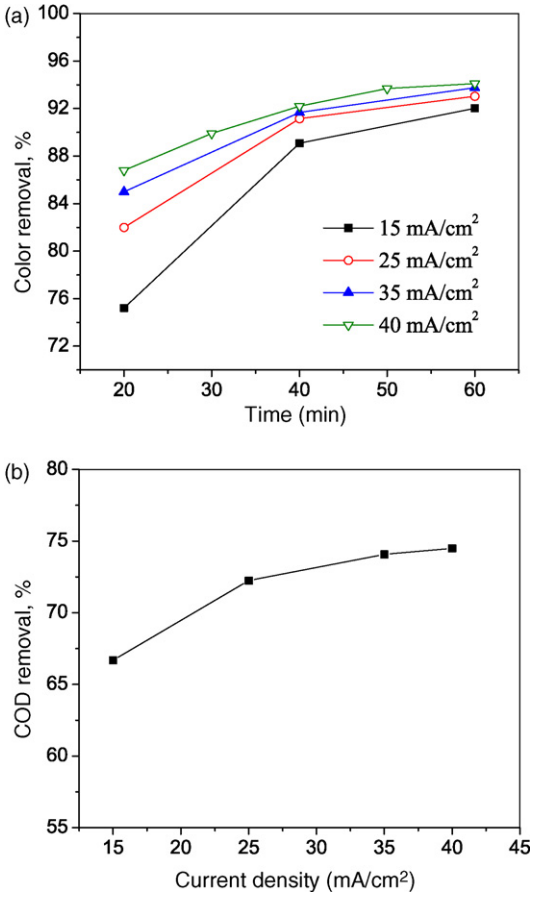

Fig. 3. Effect of current density on (a) the color removal and (b) the COD removal (ARS initial concentration, 700 mg/L; Na_2SO_4 concentration, 0.10 mol/L; pH 7).

removal efficiency after 60 min of electrolysis increased accordingly. A constant COD removal efficiency of about 74% was attained when initial pH was over 7.0, which indicates that dye could be effectively degraded in neutral medium. It is known from literature [33] that the two ionization constants, pK_{a_1} and pK_{a_2} of ARS in aqueous solution are 5.61 and 10.96, respectively. The existent form of ARS will change from H_2L^- to HL^{2-} when pH is greater than 5.6. The increase in negative charge of dye molecule makes ARS be adsorbed much more easily on the ACF anode where ARS is degraded by electrochemical oxidation.

3.1.2. Effect of current density

As shown in Fig. 3, both the color removal and the COD removal of samples exhibit a positive correlation with applied current density. After 60 min of electrolysis, the COD removal efficiency increased to 74.5% at 40 mA/cm^2 from 66.7% at 15 mA/cm^2. The results may be attributed to the increase of hydroxyl radical and $S_2O_8^{2-}$ by increasing current density. Because hydroxyl radical can be produced on the carbon felt anode surface by anodic oxidation of water according to literature [30,34,35]. In addition, Michaud et al. [36] reported that peroxodisulfate can also be generated by electrolysis in media containing sulfate ions ($2SO_4^{2-} \rightarrow S_2O_8^{2-} + 2e^-$). Therefore, on the one hand, hydroxyl radicals adsorbed on the active sites at the ACF anode surface increase with current density, which in turn would enhance the rate of direct electro-oxidation of ARS. On the other hand, the increased current density could also increase the amount of active intermediates such as hydroxyl radical and $S_2O_8^{2-}$ in the bulk solution, which would facilitate the indirect electro-oxidation of ARS.

When the current density was over 25 mA/cm^2, the degradation efficiency of dye increased slowly with current density increasing. This is because the secondary reaction of oxygen evolution is also accelerated by increasing current density. Therefore, although a larger current density is more advantageous to dye removal, a current density of 25 mA/cm^2 would be advisable in view of energy efficiency.

3.1.3. Effect of supporting electrolyte

The change in the ARS degradation efficiency caused by supporting electrolyte (Na_2SO_4) with various concentrations was investigated. As shown in Fig. 4, the color removal efficiency (Fig. 4a) and the COD removal efficiency (Fig. 4b) of all samples were almost same after 60 min of electrolysis. That is to say, the concentration of supporting electrolyte (Na_2SO_4) has a slight effect on the final degradation degree of dye. This is because the addition of Na_2SO_4 is mostly to increase solution conductivity and reduce cell voltage, and accordingly decrease

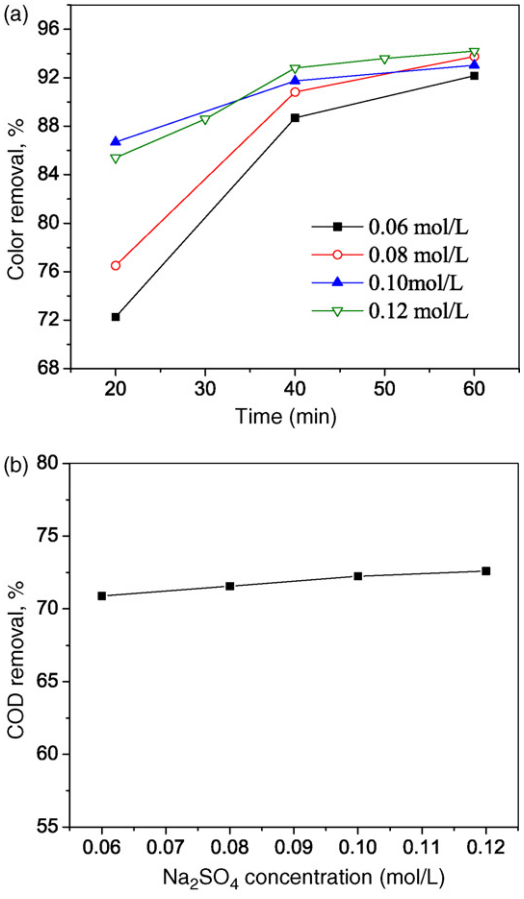

Fig. 4. Effect of Na_2SO_4 concentration on (a) the color removal and (b) the COD removal (ARS initial concentration, 700 mg/L; pH 7; current density, 25 mA/cm^2).

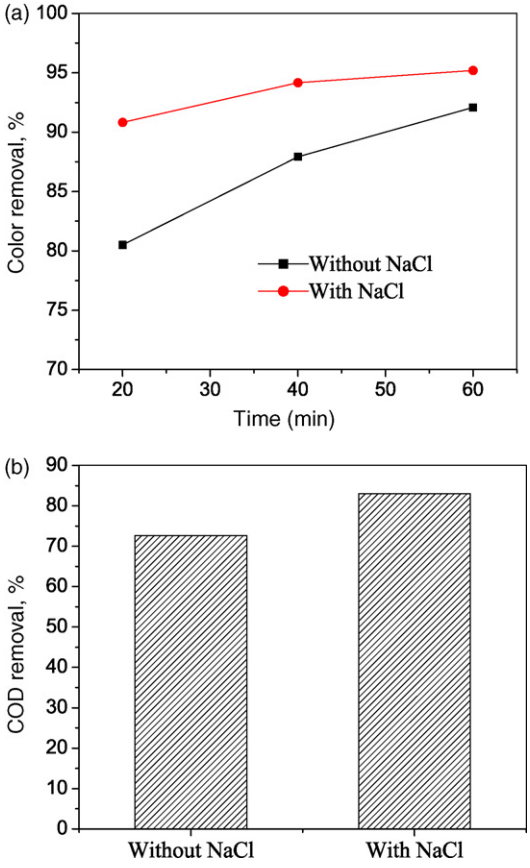

Fig. 5. Effect of the addition of NaCl on (a) the color removal and (b) the COD removal (ARS initial concentration, 700 mg/L; Na_2SO_4 concentration, 0.10 mol/L; pH 7; current density, 25 mA/cm^2).

electrical energy consumption. However, at preliminary phase (a period of less than 40 min), a relatively higher color removal efficiency was obtained when a higher concentration of Na_2SO_4 was employed. The possible reason is that the persulfate that can oxidize organic dyes may be generated in media containing sulfate ions [36]. And at the beginning of electrolysis, the amount of persulfate electrogenerated in a higher concentration of Na_2SO_4 solution is larger than that in a lower concentration of Na_2SO_4 solution. With the time of electrolysis prolonging, the different of them dwindles gradually. After all, the amount of persulfate electrogenerated was small, which cannot play a decisive role in the ARS degradation.

Fig. 5 demonstrates the presence of NaCl can improve the degradation efficiency of dye. Compared with the case without additional NaCl, the color removal efficiency and the COD removal efficiency after electrolysis for 60 min were increased by 3.1 and 10.3%, respectively. The phenomenon may be attributed to the indirect electro-oxidation of ARS by active chlorine (given by the mixture of Cl_2, HOCl and OCl^-) electrogenerated from Cl^- on the anode. However, the active chlorine just can lead partial mineralization of dyes [10,22].

In phosphate buffer solution (pH 7.0), the absorption spectrum of ARS is characterized by three bands with their maxima located at 507, 331 and 259 nm. The absorbance peak at 507 nm corresponds to the quinonyl and those at 331 and 259 nm are due to the presence of aromatic ring. During electrochemical oxidation, the chromophore of ARS, namely quinonyl, is firstly destroyed and some small aromatic molecules are generated accordingly. Only when these small aromatic molecules are degraded subsequently can the COD removal efficiency be

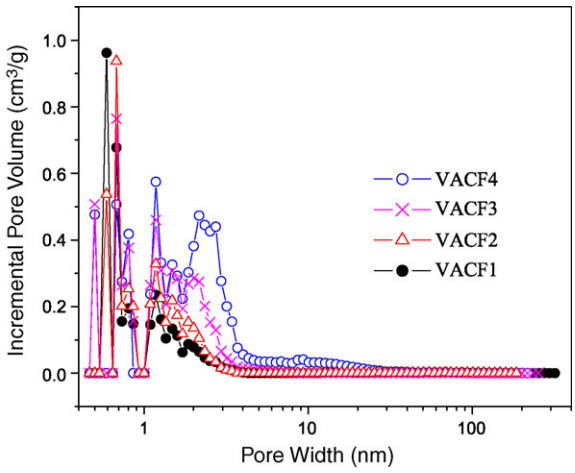

Fig. 6. Pore size distributions of VACFs by DFT method.

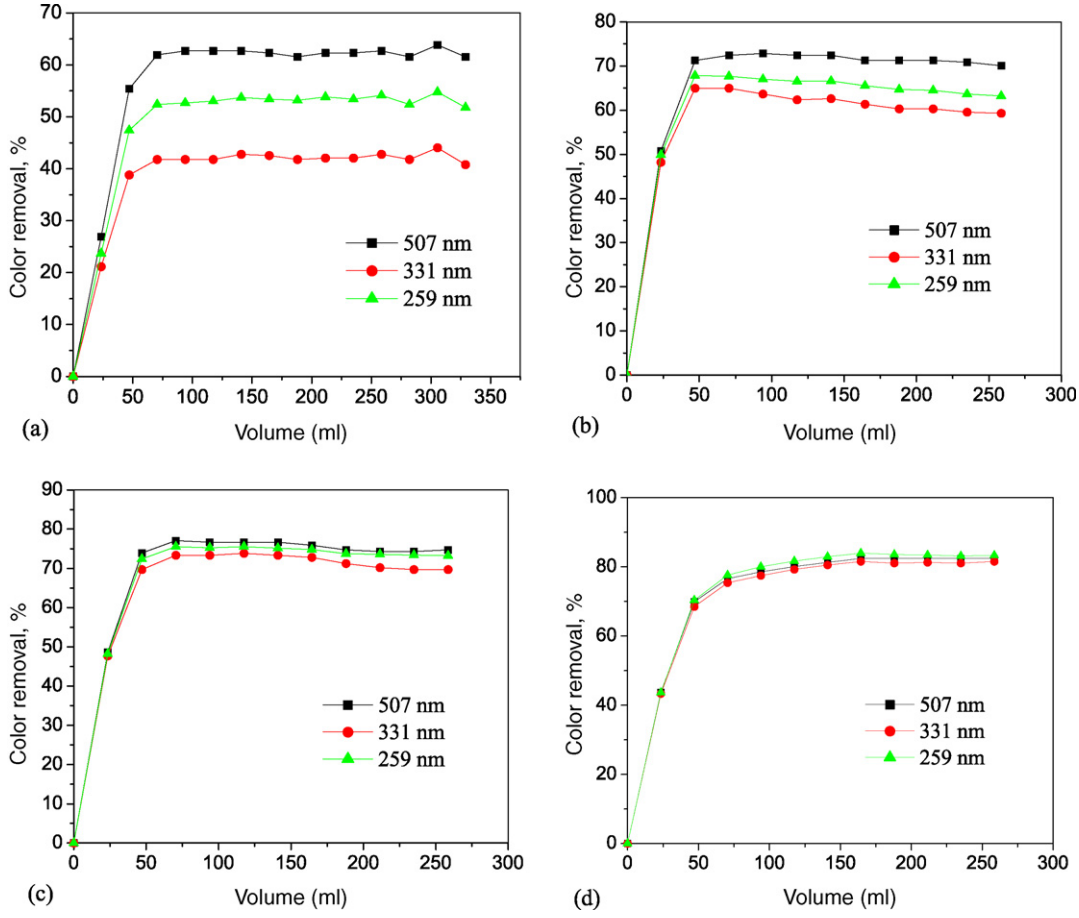

Fig. 7. Plots of color removal efficiencies vs. cumulative effluent volume using (a) VACF1, (b) VACF2, (c) VACF3, (d) VACF4 as an anode, respectively (ARS initial concentration, 200 mg/L; Na_2SO_4 concentration, 0.10 mol/L; current density, 25 mA/cm^2).

further increased. Because of this, it is clear the reason why color removal efficiency measured at 507 nm runs faster than COD removal efficiency; moreover the data of color removal efficiency measured at 331 and 259 nm can reflect the COD removal efficiency to a certain extent. So in the succedent continuous experiments, the color removal efficiencies measured at 507, 331 and 259 nm are used to evaluate the treatment effect of ARS dye wastewater.

3.2. Influence of anode structure on ARS degradation

Four ACF samples with different pore structures, namely VACF1, VACF2, VACF3 and VACF4, were prepared and used as anodes in electrochemical degradation of ARS dye. Their surface structure parameters such as BET surface area (S_{BET}), micropore surface area (S_{mic}), proportion of micropore surface area (S_{mic}/S_{BET}), average pore diameter (D), total pore volume (V_{total}), and micropore volume (V_{mic}) are listed in Table 1. The specific surface areas of these four samples are in the range of 893–1682 m^2/g. VACF1 and VACF2 possess a high percentage of microspores, with the S_{mic}/S_{BET} of 74.9 and 72%, respectively. For VACF3, the percentage of micropore is approximately identical to that of mesopore based on the S_{mic}/S_{BET} of 57.2%. VACF4 has the largest mesopore percentage in all samples with the S_{mic}/S_{BET} of only 20%. Pore size distributions of all samples are presented in Fig. 6. It is obvious that a majority of pore diameters of VACF1, VACF2 and VACF3 present a narrowly sized distribution in the range of 0.5–1.0 nm with a fairly small proportion pore diameters ranging from 1.0 to 2.0 nm. Whereas for VACF4, its pore sizes mainly distribute in the range of 2.0–4.0 nm.

The effects of anode structures on ARS removal were studied by means of continuous experiments. Fig. 7 shows plots of color removal efficiencies vs. cumulative effluent volume using VACF1, VACF2, VACF3 and VACF4 as an anode, respectively. It can be noted that in all four cases, color removal efficiencies determined at 507, 331 and 259 nm increased rapidly with cumulative effluent volume at the beginning phase and then approached a constant value. The latter phenomenon indicates that equilibrium exists between the removal of dye by electrolysis and the supplement of dye by continuously influent dye solution.

As shown in Fig. 7, a better color removal efficiency could be achieved by using an anode with higher specific surface area and mesopore percentage as expected. For example, in the case of VACF1, the color removal efficiency tested at 507 nm was only 62.7% (Fig. 7a) while that of VACF4 was 82.4% (Fig. 7d).

Table 1
Pore structure parameters of VACFs

Samples	S_{BET} (m^2/g)	S_{mic} (m^2/g)	S_{mic}/S_{BET} (%)	D (nm)	V_{total} (cm^3/g)	V_{mic} (cm^3/g)
VACF1	893.7	669.4	74.9	1.96	0.437	0.311
VACF2	1053	758.4	72.0	1.94	0.510	0.352
VACF3	1374	786.6	57.2	1.97	0.678	0.356
VACF4	1682	335.8	20.0	2.18	0.918	0.132

In addition, it can be observed that differences among color removal efficiencies determined at 507, 331 and 259 nm diminish with the increase of the specific surface area and mesopore percentage of applied VACF anode. In the case of VACF1, the difference between color removal efficiencies determined at 507 and 331 nm was of 19.9%, which was greater than that of VACF2 with a difference of 7.9%. While for VACF4, the difference dropped dramatically to only 0.9%.

It is believed that the above results are correlated with the adsorption performance of VACF anode. Indeed, ARS molecules and some intermediate products can be more effectively adsorbed and concentrated on the surface of VACF anode that possesses a higher specific surface area and mesopore percentage (e.g., VACF3 and VACF4), which would facilitates the degradation of dye. Thus, a higher ARS removal efficiency is obtained. In addition, because few aromatic intermediates would return into the solution in the above case, thereby, there is only a small difference among color removal efficiencies determined at all three absorption wavelength. In contrast, VACF anodes (e.g., VACF1 and VACF2) with low specific surface area and mesopore percentage have relatively lower adsorption capacities for ARS and intermediate products. In continuous condition, a part of aromatic intermediates would be discharged into the solution before they have been completely degraded, which results in a

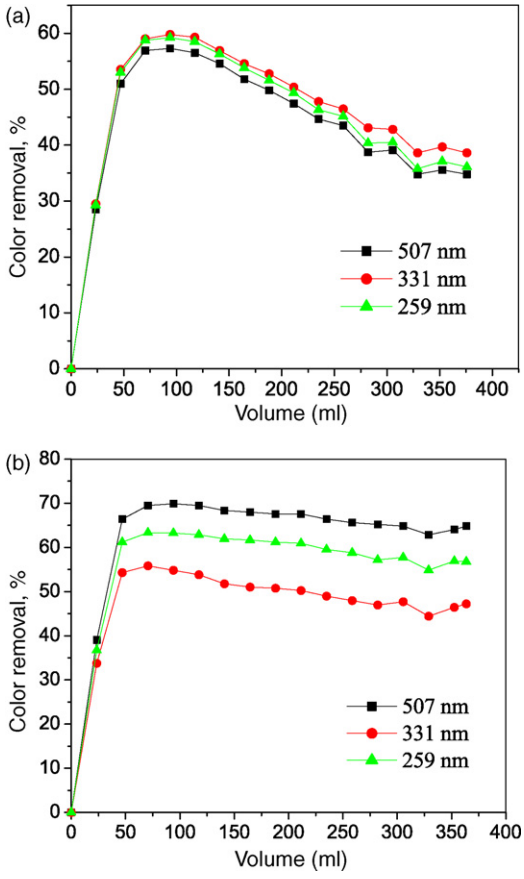

Fig. 8. Plots of color removal efficiencies vs. cumulative effluent volume using VACF5 as (a) an adsorbent and (b) an anode, respectively (ARS initial concentration, 200 mg/L; Na_2SO_4 concentration, 0.10 mol/L; current density, 25 mA/cm^2).

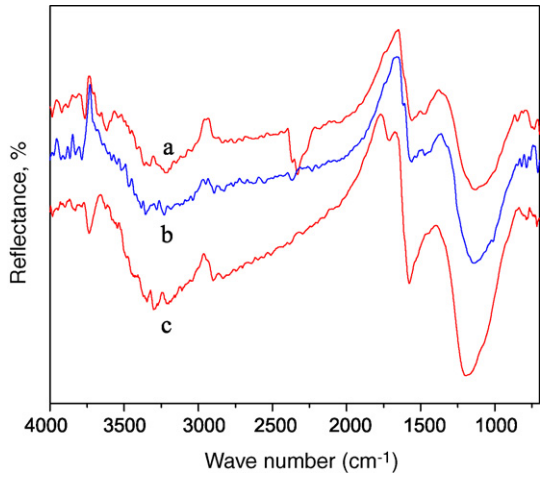

Fig. 9. IR spectra of VACFs before and after treatment of ARS dye wastewater: (a) original VACF5; (b) VACF5 after adsorption; (c) VACF5 after electrolysis.

low ARS removal efficiency and a large difference among color removal efficiencies measured at 507, 331 and 259 nm.

3.3. Surface structure of VACF anode after electrolysis

Fig. 8 presents plots of the color removal efficiencies vs. cumulative effluent volume in continuous experiment with VACF5 used as an absorbent and an anode, respectively. The pore structure parameters of VACF5 are listed in Table 2. While VACF5 was used as an absorbent (Fig. 8a), the color removal efficiencies determined at 507, 331 and 259 nm continuously increased and reached a maximum when a saturation adsorption was achieved. Then color removal efficiencies decreased rapidly, since no more dye molecule could be adsorbed by the VACF adsorbent after the saturation adsorption. Additionally, as no ARS degradation would take place in the adsorption process, the color removal efficiencies detected at 507, 331 and 259 nm are almost alike. In the case of VACF5 used as an anode (Fig. 8b), there is no saturation adsorption because ARS adsorbed on the VACF anode could be decomposed by electrolysis. That is to say, a synergistic effect of adsorption and

Table 2
Pore structure parameters of VACFs before and after treatment of ARS dye wastewater

Samples	S_{BET} (m^2/g)	S_{mic} (m^2/g)	D (nm)	V_{total} (cm^3/g)	V_{mic} (cm^3/g)
Original VACF5	1256.5	1011.5	1.94	0.609	0.470
VACF5 anode after electrolysis	1196.5	938.9	1.95	0.583	0.428
VACF5 adsorbent after adsorption	986.2	753.2	1.96	0.482	0.350

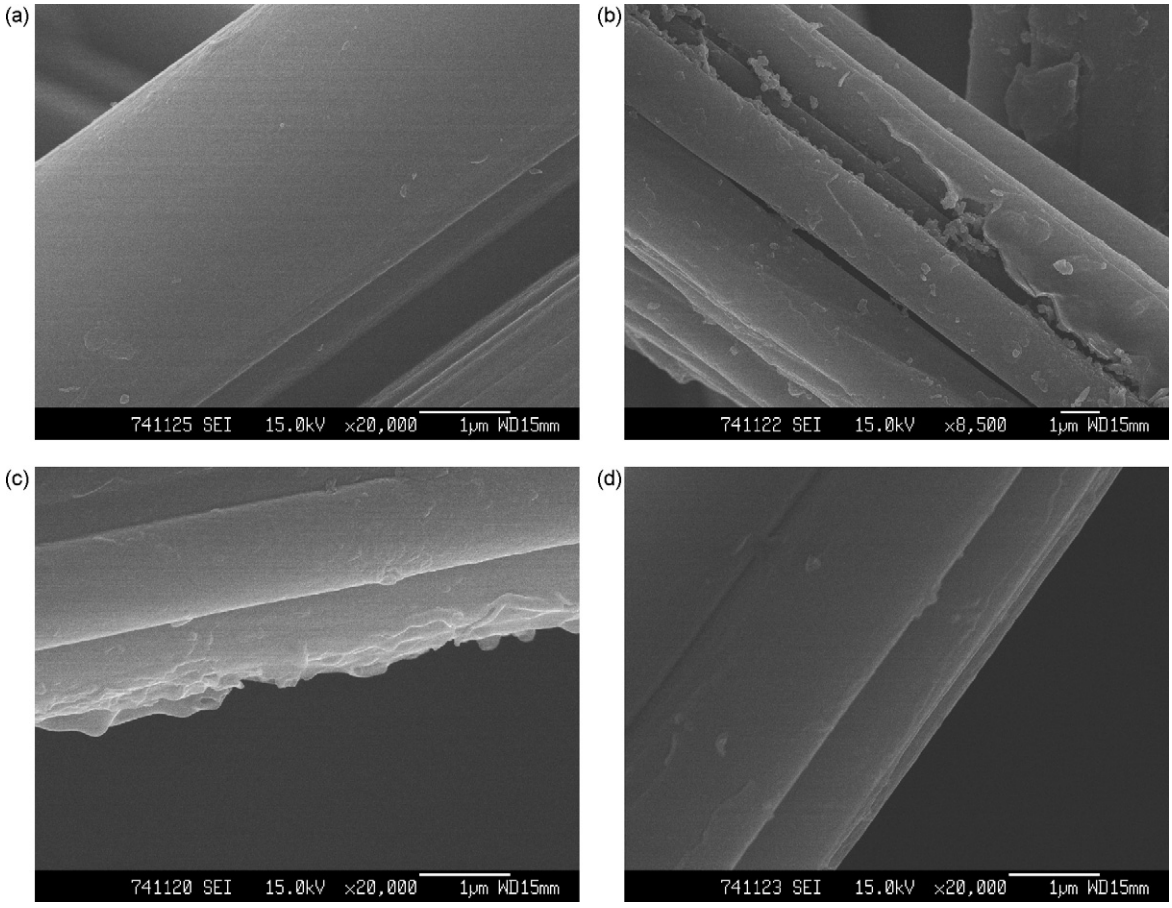

Fig. 10. The SEM micrographs of VACFs before and after treatment of ARS dye wastewater: (a) original VACF5; (b and c) VACF5 after adsorption; (d) VACF5 after electrolysis.

electrolysis exists when ACF is used as an anode to treat dye wastewater.

VACF adsorbent and VACF anode after treatment of dye wastewater were washed with distilled water and dried in vacuum, their surface structure were analyzed by means of ATR/FTIR spectroscopy, SEM and nitrogen adsorption method.

ATR/FTIR was employed to analyze changes in functional groups of the VACF samples. Fig. 9 shows the ATR/FTIR spectra of VACFs before and after treatment of ARS wastewater. For original VACF5 (a in Fig. 9), there are four absorption bands at around 1130, 1560, 3250 and 2300 cm^{-1}, corresponding to $\nu_{C–O}$ in hydroxybenzene, $\nu_{C=C}$ in aryl, $\nu_{O–H}$ in hydroxybenzene and $\nu_{C\equiv N}$, respectively. This is a direct indication of the presence of abundant phenolic –OH groups and a small quantity of –C≡N groups on the surface of VACF. So it can be deduced that VACF5 has a good adsorption performance for polar dye molecules. After dye adsorption, there was no change between IR spectra of original VAF5 (a in Fig. 9) and spent VACF5 (b in Fig. 9) except a slight decrease in the relative intensity of the absorption band at about 2300 cm^{-1}. For the sample of VACF5 after electrolysis (c in Fig. 9), the increase in relative intensities of the three main absorption bands at about 1130, 1560 and 3250 cm^{-1} indicates an increase in the content of phenolic –OH groups on VACF5 anode. Besides, the peak at about 2300 cm^{-1} disappeared with the appearance of a new one at about 1700 cm^{-1}. This is because that part of –C≡N groups on the VACF were hydrolyzed and some –COOH groups were produced after electrolysis. In conclusion, the amount of oxygen-containing groups on the VACF surface was increased in the process of dye electrochemical treatment, which would in turn enhance the adsorption capacity of VACF for polar dye molecules.

SEM micrographs of VACFs before and after treatment of ARS wastewater are shown in Fig. 10. Compared with original VACF5 (Fig. 10a), the surface of spent VACF5 adsorbent was covered with a layer of membrane-like substance after adsorption (Fig. 10b and c). This phenomenon was possibly due to the formation of floccules induced by congregation of ARS molecules when the solution pH was adjusted to about 7. The floccules would block the pores of the VACF adsorbent, so that the adsorption capability of VACF for ARS was weaken. In contrast, no visual changes can be observed between VACF5 anode after electrolysis (Fig. 10d) and original VACF5 (Fig. 10a). The results suggest that ARS molecules adsorbed on VACF anode were degraded by electrochemical oxidation. At this point, the VACF anode could be regenerated at real time during the electrolysis process. All the information demonstrated in Fig. 10 is consistent with that in Fig. 8.

The above conclusions can be also confirmed by the pore structure parameters of VACFs before and after treatment of ARS dye wastewater, as listed in Table 2. The VACF5 anode underwent a slight decrease of only 4.8% in BET surface area and 4.3% in total pore volume after electrolysis treatment of dye wastewater. However, when VACF5 was used as an adsorbent, a 21.5% decrease in BET surface area and a 20.9% decrease in total pore volume happened, which means that a large amount of pores on VACF were occupied by dye molecules.

4. Conclusions

In the electrochemical degradation of ARS by using ACF as an anode, electrolytic conditions such as initial pH of solution, current density and supporting electrolyte and anodic structure all influence the degradation of ARS.

Increasing the initial pH and the current density will lead to a corresponding increase in the ARS removal. The addition of NaCl can also enhance the degradation efficiency of ARS. Under the optimum condition, a color removal efficiency of 95% and a COD removal efficiency of over 80% within 60 min can be obtained by using ACF as an anode.

ACF anode that has a higher specific surface area and mesopore percentage can more effectively adsorb and concentrate ARS molecules on its surface from the solution, which will facilitate the electro-oxidation degradation of ARS. As a result, a higher ARS removal efficiency can be obtained by using an ACF anode with high surface area and high mesopore percentage.

Acknowledgements

This work is financially supported by Natural Science Foundation of Guangdong Province (5003270) and Leading Science Project of Guangdong Province (2005B10301005).

References

[1] J.X. Yan, Q.L. Cheng, A review on the treatment technology of dyeing wastewater, Dyestuffs Coloration 44 (2007) 48–51.
[2] E. Oguz, B. Keskinler, Z. Celik, Ozonation of aqueous Bomaplex Red CR-L dye in a semi-batch reactor, Dyes Pigments 64 (2005) 101–108.
[3] D.K. Lee, I.C. Cho, G.S. Lee, S.C. Kim, D.S. Kim, Y.K. Yang, Catalytic wet oxidation of reactive dyes with H_2/O_2 mixture on Pd-Pt/Al_2O_3 catalysts, Sep. Purif. Technol. 34 (2004) 43–50.
[4] Y. Liu, D.Z. Sun, Development of Fe_2O_3–CeO_2–TiO_2/γ-Al_2O_3 as catalyst for catalytic wet air oxidation of methyl orange azo dye under room condition, Appl. Catal. B Environ. 72 (2007) 205–211.
[5] O.Ö. Söğüt, M. Akgün, Treatment of textile wastewater by SCWO in a tube reactor, J. Supercrit. Fluid 43 (2007) 106–111.
[6] R.S. Yuan, R.B. Guan, W.Z. Shen, J.T. Zheng, Photocatalytic degradation of methylene blue by a combination of TiO_2 and activated carbon fibers, J. Colloid Interface Sci. 282 (2005) 87–91.
[7] L. Rizzo, J. Koch, V. Belgiorno, M.A. Anderson, Removal of methylene blue in a photocatalytic reactor using polymethylmethacrylate supported TiO_2 nanofilm, Desalination 211 (2007) 1–9.
[8] A. Fernandes, A. Morão, M. Magrinho, A. Lopes, I. Goncalves, Electrochemical degradation of C.I. Acid Orange 7, Dyes Pigments 61 (2004) 287–296.
[9] A.S. Koparal, Y. Yavuz, C. Gürel, Ü.B. Öğütveren, Electrochemical degradation and toxicity reduction of C.I. Basic Red 29 solution and textile wastewater by using diamond anode, J. Hazard. Mater. 145 (2007) 100–108.
[10] D. Rajkumar, B.J. Song, J.G. Kim, Electrochemical degradation of Reactive Blue 19 in chloride medium for the treatment of textile dyeing wastewater with identification of intermediate compounds, Dyes Pigments 72 (2007) 1–7.
[11] N. Mohan, N. Balasubramanian, C. Ahmed Basha, Electrochemical oxidation of textile wastewater and its reuse, J. Hazard. Mater. 147 (2007) 644–651.
[12] P. Ronaldo, P. Patricio, DeA. Adalgisa, R. Juan, D. Nelson, Electrochemically assisted photocatalytic degradation of reactive dyes, Appl. Catal. B Environ. 22 (1999) 83–90.
[13] Y. Xiong, P.J. Strunk, H.Y. Xia, X.H. Zhu, H.T. Karlsson, Treatment of dye wastewater containing Acid Orange II using a cell with

three-phase three-dimensional electrode, Water Res. 35 (2001) 4226–4230.
[14] Z. Zainal, C.Y. Lee, M.Z. Hussein, A. Kassim, N.A. Yusof, Electrochemical-assisted photodegradation of mixed dye and textile effluents using TiO_2 thin films, J. Hazard. Mater. 146 (2007) 73–80.
[15] Z.M. Shen, D. Wu, J. Yang, T. Yuan, W.H. Wang, J.P. Jia, Methods to improve electrochemical treatment effect of dye wastewater, J. Hazard. Mater. B131 (2006) 90–97.
[16] B.K. Körbahti, Response surface optimization of electrochemical treatment of textile dye wastewater, J. Hazard. Mater. 145 (2007) 277–286.
[17] N. Daneshvar, A.R. Khataee, A.R. Amani Ghadim, M.H. Rasoulifard, Decolorization of C.I. Acid Yellow 23 solution by electrocoagulation process: investigation of operational parameters and evaluation of specific electrical energy consumption (SEEC), J. Hazard. Mater. 148 (2007) 566–572.
[18] H.S. Awad, N. Abo Galwa, Electrochemical degradation of Acid Blue and Basic Brown dyes on Pb/PbO_2 electrode in the presence of different conductive electrolyte and effect of various operating factors, Chemosphere 61 (2005) 1327–1335.
[19] J.S. Chen, M.C. Liu, J.D. Zhang, Y.Z. Xian, L.T. Jin, Electrochemical degradation of bromopyrogallol red in presence of cobalt ions, Chemosphere 53 (2003) 1131–1136.
[20] D. Dogan, H. Turkdemir, Electrochemical oxidation of textile dye indigo, J. Chem. Technol. Biotechnol. 80 (2005) 916–923.
[21] N. Mohan, N. Balasubramanian, In situ electrocatalytic oxidation of acid violet 12 dye effluent, J. Hazard. Mater. B136 (2006) 239–243.
[22] F.H. Oliveira, M.E. Osugi, F.M.M. Paschoal, D. Profeti, P. Olivi, M.V.B. Zanoni, Electrochemical oxidation of an acid dye by active chlorine generated using $Ti/Sn_{(1-x)}Ir_xO_2$ electrodes, J. Appl. Electrochem. 37 (2007) 583–592.
[23] E. Butron, M.E. Juarez, M. Solis, M. Teutli, I. Gonzalez, J.L. Navad, Electrochemical incineration of indigo textile dye in filter-press-type FM01-LC electrochemical cell using BDD electrodes, Electrochim. Acta 52 (2007) 6888–6894.
[24] C. Saez, M. Panizza, M.A. Rodrigo, G. Cerisola, Electrochemical incineration of dyes using a boron-doped diamond anode, J. Chem. Technol. Biotechnol. 82 (2007) 575–581.
[25] P. Canizares, A. Gadri, J. Lobato, B. Nasr, R. Paz, M.A. Rodrigo, C. Saez, Electrochemical oxidation of azoic dyes with conductive-diamond anodes, Ind. Eng. Chem. Res. 45 (2006) 3468–3473.
[26] M. Panizza, G. Cerisola, Electrocatalytic materials for the electrochemical oxidation of synthetic dyes, Appl. Catal. B Environ. 75 (2007) 95–101.
[27] X.M. Chen, F.R. Gao, G.H. Chen, Comparison of Ti/BDD and $Ti/SnO_2–Sb_2O_5$ electrodes for pollutant oxidation, J. Appl. Electrochem. 35 (2005) 185–191.
[28] P. Tissot, M. Fragniere, Anodic oxidation of cyanide on a reticulated three-dimensional electrode, J. Appl. Electrochem. 24 (1994) 509–512.
[29] L. Fan, Y.W. Zhou, W.S. Yang, G.H. Chen, F.L. Yang, Electrochemical degradation of aqueous solution of Amaranth azo dye on ACF under potentiostatic model, Dyes Pigments 76 (2008) 440–446.
[30] A.-M. Wang, J.-H. Qu, L.-L. Song, J. Ru, Electrochemical generation of hydroxyl radicals for Acid Red B degradation by activated carbon fiber electrodes, Acta Chim. Sinica 64 (2006) 767–771.
[31] F.Y. Yi, S. Chen, Electrochemical treatment of alizarin red S dye wastewater using an activated carbon fiber as anode material, J. Porous Mater. (2007), doi:10.1007/s10934-007-9134-2.
[32] Editorial Committee of Monitoring and determination methods for water and wastewater, SEPA (State Environmental Protection Administration of China), Monitoring and Determination Methods for Water and Wastewater, China Environmental Science Press, Beijing, 2002, p. 211.
[33] P.S. Cong, Z.L. Zhu, T.H. Li, The determination of ionization constants of polyprotic by using evolving factor analysis and pH-spectrophotometric data, Chem. J. Chinese U. 15 (1994) 1292–1296.
[34] C.Y. Zheng, F.Y. Yi, S. Chen, Study on treatment of the wastewater containing phenol with ACF electrode method, J. Funct. Mater. 38 (3) (2007) 451–454.
[35] A.M. Polcaro, S. Palmas, Electrochemical oxidation of chlorophenols, Ind. Eng. Chem. Res. 36 (5) (1997) 1791–1798.
[36] P.-A. Michaud, E. Mahe, W. Haenni, A. Perret, Ch. Comninellis, Preparation of peroxodisulfuric acid using boron-doped diamond thin film electrodes, Electrochem. Solid State 3 (2) (2000) 77–79.